X-ray imaging and diffraction from surface phonons on GaAs

W. Sauer,[a] M. Streibl, T. H. Metzger, A. G. C. Haubrich, S. Manus, A. Wixforth, and J. Peisl
Sektion Physik and CeNS, Ludwig-Maximilians-Universität München, D-80539 München, Germany

A. Mazuelas, J. Härtwig, and J. Baruchel
ESRF, BP 220, F-38043 Grenoble, France

(Received 3 March 1999; accepted for publication 21 July 1999)

Surface acoustic waves (SAWs) are excited on the GaAs (001) surface by using interdigital transducers, designed for frequencies of up to 900 MHz. The emitted phonons with wavelengths down to 3.5 μm are visualized and characterized by combined x-ray diffraction techniques. Using stroboscopic topography, the SAW emission of a parallel and a focusing transducer geometry are imaged. High-resolution x-ray diffraction profiles show up to 12 phonon-induced satellite reflections besides the GaAs (004) reflection, with a width of 9 arcsec each. The diffraction pattern is simulated numerically, applying the kinematical scattering theory to a model crystal. From fits to measured diffraction profiles at different excitation voltages, the SAW amplitudes were calculated and found to be in the sub-nm range. © *1999 American Institute of Physics.* [S0003-6951(99)01538-7]

Phonon excitations in crystals have been investigated for some time by x-ray, neutron, and light diffraction methods. Of interest is the visualization of the wave field and the determination of the amplitude of the surface wave. Possible applications are tunable monochromators for x rays[1] or neutrons.[2] Surface acoustic waves (SAWs) on the most prominent SAW material $LiNbO_3$ were studied by different x-ray methods: topography in the MHz frequency region[3,4] and at 300 MHz.[5] Under grazing incidence angles, x-ray beam modulation was demonstated[6] and the influence on surface reflections was shown.[7,8]

In this letter, we describe diffraction experiments under SAW excitation on GaAs. The orientation of the surface is (001) and the direction of SAW propagation is [110]. The efficiency of both parallel and focusing transducers is demonstrated and it is shown that the mechanical amplitudes below 1 nm can be detected. Due to its properties as a direct band-gap semiconductor, GaAs is a very promising material for further SAW applications,[9] as well as a material for a SAW-tunable x-ray monochromator.

The synchrotron x-ray source at the European Synchrotron Radiation Facility (ESRF), Grenoble, offers the possibility to perform time-resolved experiments. In the 16-bunch mode, out of 992 positions, only 16 uniformly distributed positions of the ring are populated by electron bunches. One bunch packet passes the insertion device in less than 100 ps. In this mode of operation, the source provides well-defined x-ray pulses with a repetition frequency of 5.68 MHz. As shown in Fig. 1, the driver frequency of the synchrotron was multiplied 102 times by a phase-locked loop (PLL), amplified, and used as excitation frequency for the SAW device. This implicates that the surface wave is always in phase to the light pulses and one obtains a standing image of the propagating wave. The large x-ray spot size of $45\times15\,\mathrm{mm}^2$ at the topography beamline allows us to illuminate the whole sample surface. For both topography and high-resolution diffraction, the energy was adjusted by a double-crystal Si(111) monochromator to 12 keV. Using the symmetric (004) reflection of the GaAs single crystal, the penetration depth of the x rays is below 5 μm and about the same as the penetration depth of the surface acoustic wave.

In Fig. 2(a), an image obtained from a sample with a parallel transducer structure is shown. Due to the projection of the sample surface at the Bragg angle of 20.7°, the image is compressed and tilted in the vertical direction. The SAW-propagation direction [110] is indicated, and the SAW is imaged by a strain-induced variation in contrast with the same period as the wavelength, $\Lambda_{SAW}=5\,\mu$m. The vertical line on the right marks the edge of the transducer. Beyond the SAW-induced contrast variation, the defect structure of the substrate becomes visible. It represents a dislocation network typical for Bridgman-grown GaAs, which is distributed over the whole crystal. Figure 2(b) shows an image of the excited waves from a focusing transducer structure in the form of a segment of a circle. The transducer is located again at the right edge of the image and the SAW is focused to a spot 1000 μm away on the left side of the image, marked by two arrows. The magnification shows the focusing wave fronts, formed in front of the transducer structure.

Besides topography, high-resolution reciprocal space intensity maps were collected at the GaAs (004) reflection with

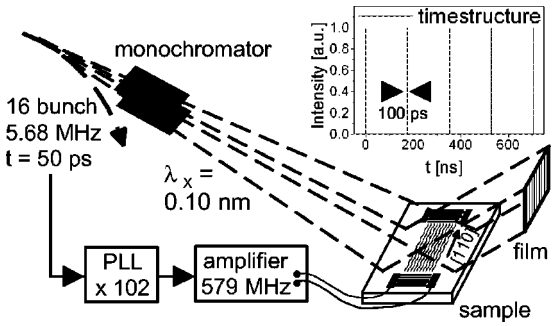

FIG. 1. Experimental setup for imaging surface waves by x-ray topography.

[a]Electronic mail: wsauer@lrz.uni-muenchen.de

 © 1999 American Institute of Physics

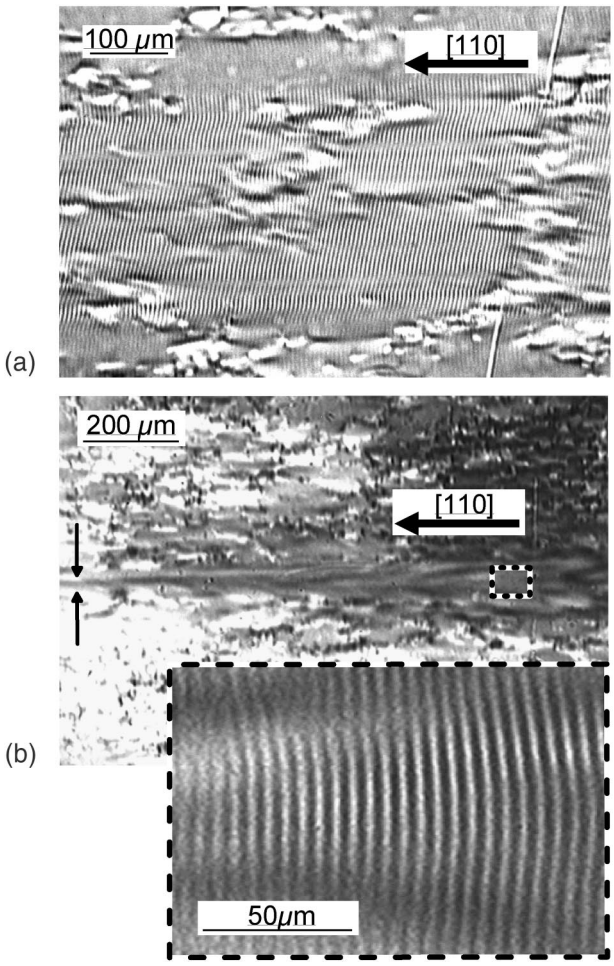

FIG. 2. X-ray topographs of GaAs [reflection (004), $\lambda = 0.10$ nm] with SAW excitation, emitted from a parallel (a) and a focusing (b) transducer on the;right, propagating along [110], and magnified image of the indicated area in (b).

excitation of surface waves with a wavelength of $\Lambda_{SAW} = 3.5\ \mu$m. For this purpose, a four-crystal setup including a Si(111) double monochromator, the sample crystal, and a Si(111) analyzer was used. For a detailed description see Ref. 10. In order to illuminate only the fraction of the acoustic path on the sample surface, the beam size was restricted to a spot of $0.2 \times 0.2\ \text{mm}^2$. In comparison to Fig. 1, the sample orientation is now turned by 90°. Thus, rocking the sample and the analyzer stage allows us to record mappings in the area including the direction of SAW propagation ($\mathbf{Q}_\parallel$), and the direction perpendicular to it ($\mathbf{Q}_\perp$). For comparison, logarithmically scaled mappings of the same region without and with SAW excitation are shown in Fig. 3. The mappings show the GaAs reflection with a width of 9 arcsec in the center, where $\mathbf{Q} = \mathbf{K}$ holds, with $\mathbf{Q}$ being the diffraction vector and $\mathbf{K}$ the reciprocal lattice vector. Due to the wavelength spread a streak along $\mathbf{Q}_\perp$ is visible. Orientated oblique to this streak, streaks from the Darwin curve of the monochromator and the analyzer crystal are also clearly visible. Under excitation of a SAW with a wave vector $\mathbf{q}_{SAW}$, symmetric satellite peaks along $\mathbf{Q}_\parallel$ at the positions $\mathbf{Q} = \mathbf{K} + N \cdot \mathbf{q}_{SAW}$ appear. By increasing the amplitude of the SAW, up to 12 side peaks on every side of the (004) reflection were resolved. With an amplitude of up to 50% of the (004) peak, they dominate the diffraction image and even suppress the sample streak.

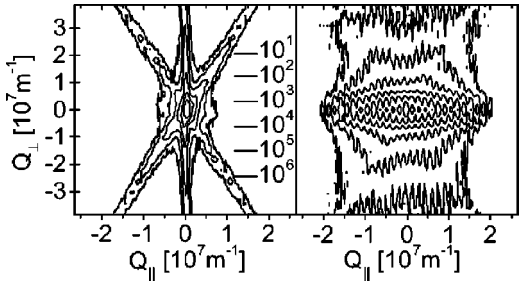

FIG. 3. Log-scaled, reciprocal space intensity map at the GaAs (004) reflection without (left) and with (right) SAW excitation.

For an evaluation of the diffraction data, the scattering process was treated kinematical and the Fourier transform over the crystal lattice was performed numerically. The x-ray scattering amplitude is given by the Fourier transform of the electron density and can be written in the general form:

$$F(\mathbf{Q}) = \sum_{i=1}^{N} f_i(\mathbf{Q}) e^{i\mathbf{Q}\cdot\mathbf{r}_i}. \tag{1}$$

The sum runs over all N atoms in the crystal, where f_i is the atomic form factor and $\mathbf{r}_i$ is the position of the atom i. The sum is calculated at each point $\mathbf{Q}$ along $\mathbf{Q}_\parallel$. With surface phonons of Rayleigh type, propagating along $\mathbf{Q}_\parallel$, the transversal displacements of the atoms are along $\mathbf{Q}_\perp$ and the longitudinal displacements are along $\mathbf{Q}_\parallel$. The third coordinate remains constant. The displacement field can be calculated[11] and is introduced in the model for the calculation of the scattering amplitude. To restrict the sum on a reasonable number of Fourier terms, the atoms are grouped to cells, which contain 5 elementary cells along $\mathbf{Q}_\parallel$ and 10 along $\mathbf{Q}_\perp$. The third direction can be ignored, because the diffraction vector $\mathbf{Q}$ has no component in this direction. Thus, the Fourier sum of Eq. (1) can be written in the following way:

$$F(\mathbf{Q}) = \sum_{i=1}^{N_S} f_S(\mathbf{Q}) e^{i\mathbf{Q}\cdot(\mathbf{r}_S + \mathbf{u}(\mathbf{r}_S))}. \tag{2}$$

Here the sum extends over N_S cells. f_S denotes the structure factor of one cell at the position $\mathbf{r}_S$. The displacement of the SAW is taken into account by adding the displacement vector $\mathbf{u}_S(\mathbf{r}_S)$ at each position of a cell. The structure factor f_S of the cell is calculated by summing over all the atoms inside:

$$f_S(\mathbf{Q}) = \sum_{i=1}^{N_C} f_i(\mathbf{Q}) e^{i\mathbf{Q}\cdot\mathbf{r}_i}. \tag{3}$$

The comparatively small displacements due to the SAW within one cell of the specified size can be neglected because the total amplitude of the SAW over its wavelength of some microns is below 1 nm.

With this concept, we are able to calculate the scattering pattern for the performed scans numerically by summing over about $N_S = 2.5 \times 10^6$ cells. Periodic boundary conditions along $\mathbf{Q}_\parallel$ have to be considered, which leads to a sum of cells along a length of multiples of Λ_{SAW} in this direction. Of course, the width of the peaks in the calculation depends on the number of scattering cells along $\mathbf{Q}_\parallel$, which were used. To match the measured width of 9 arcsec, which is limited

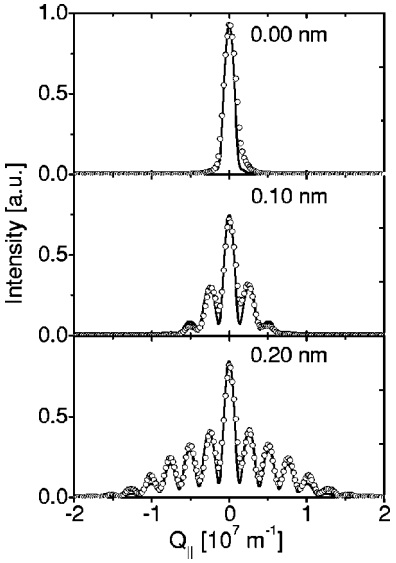

FIG. 4. Measured cuts through reciprocal space maps along $\mathbf{Q}_{\parallel}$ (points) together with simulations (lines). The SAW amplitude is changed by a linear increase of the excitation voltage from top to bottom.

by the resolution of the experimental setup, it is sufficient to sum over a number of cells equivalent to the length of $2\Lambda_{\mathrm{SAW}}$.

Along $\mathbf{Q}_{\perp}$, a sum of cells according to a length of 4.5 μm from the crystal surface is required, because this is approximately the x-ray penetration depth. Using the optimized routines implemented in the software package DISCUS,[12] the calculation is performed in less than an hour. In Fig. 4, the results of calculations for SAW amplitudes of 0, 0.1 nm and 0.2 nm are shown together with measured $\mathbf{Q}_{\parallel}$ scans at linear increased excitation voltages.

In summary, the experiment demonstrates the potential of imaging surface waves on GaAs both in direct and in reciprocal space. By topography, the efficiency of focusing transducers was probed. As there exists the technology for structurizing the GaAs surface, a further application will be the imaging of SAW amplitude and velocity changes by interacting with beam-steering structures in the path of the SAW and with overlays. By high-resolution diffraction with an x ray of small spot size, the amplitude of the SAW can be measured with a high lateral resolution, even below surface layers.

One of the authors (W.S.) acknowledges support by the German–Israelian Foundation under Project No. I-006-401.02/95.

[1] K.-D. Liss, A. Magerl, R. Hock, B. Waibel, and A. Remhof, Proc. SPIE **3451**, 14 (1998).
[2] R. Hock, T. Vogt, J. Kulda, Z. Mursic, H. Fuess, and A. Magerl, Z. Phys. B **90**, 143 (1993).
[3] R. W. Whatmore, P. A. Goddard, B. K. Tanner, and G. F. Clark, Nature (London) **299**, 44 (1982).
[4] H. Cerva and W. Graeff, Phys. Status Solidi A **82**, 35 (1984).
[5] E. Zolotoyabko, D. Shilo, W. Sauer, E. Pernot, and J. Baruchel, Appl. Phys. Lett. **73**, 16 (1998).
[6] D. V. Roschupkin, I. A. Schelokov, R. Tucoulou, and M. Brunel, IEEE Trans. Ultrason. Ferroelectr. Freq. Control **42**, 127 (1995).
[7] W. Sauer, T. H. Metzger, J. Peisl, Y. Avrahami, and E. Zolotoyabko, Nuovo Cimento D **19**, 455 (1997).
[8] W. Sauer, T. H. Metzger, J. Peisl, Y. Avrahami, and E. Zolotoyabko, Physica B **248**, 358 (1998).
[9] C. Rocke, S. Zimmermann, A. Wixforth, and J. P. Kotthaus, Phys. Rev. Lett. **78**, 4099 (1997).
[10] A. Mazuelas, S. Milita, J. Härtwig, J. Baruchel, T. Baumbach, and B. Capelle, J. Phys. D: Appl. Phys. (to be published).
[11] A. A. Oliner, *Acoustic Surface Waves* (Springer, Berlin, 1978).
[12] Th. Proffen and R. B. Neder, J. Appl. Crystallogr. **30**, 171 (1997).